# Solar activity during the deep minimum of 2009

Janusz Sylwester[1], Marek Siarkowski[1], Szymon Gburek[1], Magdalena Gryciuk[1], Anna Kępa[1], Mirosław Kowaliński[1], Tomek Mrozek[1,2], Kenneth J.H. Phillips[3], Piotr Podgórski[1] and Barbara Sylwester[1]

1. Space Research Centre, Solar Physics Division
   Kopernika 11, 51–622 Wrocław, Poland
2. Astronomical Institute, Wrocław University
   Kopernika 11, 51–622 Wrocław, Poland
3. Earth Sciences Department, Natural History Museum
   London, SW7 5BD, UK

We discuss the character of the unusually deep solar activity minimum of 2009 between Solar Cycles 23 and 24. Levels of solar activity in various parts of the solar atmosphere – photosphere, chromosphere, transition region, and corona – were observed to be at their lowest for a century. The soft X-ray emission from the corona (hot outer part of the Sun's atmosphere) was measured throughout most of 2009 with the Polish-built SphinX spectrophotometer. Unlike other X-ray monitoring spacecraft, this sensitive spacecraft-borne instrument was able to continue measurements throughout this extended period of low activity.

## 1 Introduction

For over 170 years the Sun's activity has been known to rise and fall in an approximately 11-year cycle, with the frequency of flares, coronal mass ejections and other energetic phenomena peaking at or around each solar maximum and falling off at solar minimum. Sunspots are the most obvious indicator of magnetic activity on the Sun's surface photosphere, appearing in large numbers at maximum and all but disappearing at minimum. But the behaviour of our host star is not quite predictable and the most recent solar minimum was surprisingly deep and long, finally bottoming out around late 2008 and early 2009. This was shown by the familiar Wolf sunspot number as well as ultraviolet and other activity indicators. The sunspot number is plotted in Fig. 1 (left panel) for Cycles 23 and 24, with background X-ray image showing a decaying, one-month-old active region on its second rotation across the visible solar disk. For a recent review, see Hathaway (2010). A primary driver for solar activity cycles is believed to be a dynamo mechanism which gives rise to large-scale solar magnetism in the solar equatorial activity belt (roughly between latitudes 35°S and 35° N). New-cycle active regions are born at high latitudes at a time when the sunspots of the previous cycle are still appearing close to solar equator. This equator-ward drift of the active-latitude belt is clearly seen in a so-called butterfly diagram showing sunspots, or better still in a magnetic butterfly diagram (cf. Fig. 1, centre panel). The magnetic butterfly diagram also shows the weak surface fields being carried toward the poles by a meridional flow at the surface. The strength and structure of the meridional flow varies substantially over the course of each sunspot

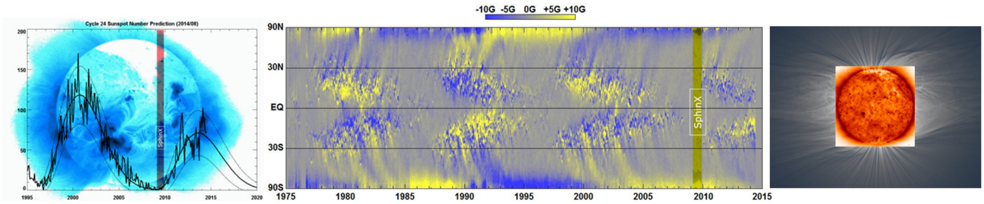


Fig. 1: **Left**: Actual and predicted sunspot numbers with the period of SphinX measurements indicated (from http://solarscience.msfc.nasa.gov/images/ssn_predict_l.gif). **Centre**: Synoptic magnetogram of the radial component of the solar surface magnetic field. Magnetic polarities are indicated by the yellow and blue colours. The central latitude region (latitudes 35 South to 35 North) is associated with sunspots. A reversal of magnetic polarity at polar latitudes occurs at approximately the time of sunspot maximum. **Right**: Enhanced image of the white-light minimum corona on 22nd July 2009 (Habbal et al., 2010). In the insert the X-ray *Hinode* XRT image of the inner corona formed at temperatures of around $1.1 \times 10^6$ K (1.1 MK) obtained using the Ti_poly filter is shown.

cycle and from one sunspot cycle to the next. The frequency of flares, chromospheric active region (or plage) area and the other indices vary in a like manner to the Wolf sunspot number as do the general level of X-ray and extreme ultraviolet (EUV) emission and the area covered by open magnetic field regions called coronal holes which occupy a large part of the solar disk around solar minimum. However, some other minor activity processes in the solar atmosphere do not show a dependence on the overall activity level. These include the X-ray bright points scattered all over the solar disk as well as micro-flares and possibly other tiny energy release processes occurring below the threshold of spacecraft instruments. Large-scale coronal structures are also prominent in total solar eclipse images made at the time of minimum activity, as can be seen in the right panel of Fig. 1. Sometimes these structures are visible at the Sun's edge (or limb) forming a helmet-shape with a prominence, bright in the light of the red H$\alpha$ line.

## 2 Was the last solar minimum unique?

In order to present the evidence, we need to compare the 2009 minimum with previous ones in terms of appropriately selected activity indices. The most used index has been the Wolf sunspot number. Records show a similarly low minimum in 1913 (between activity cycles 13 and 14). Another frequently used index for characterizing solar minima is "days with no spots (DWNS)" (de Toma, 2011) (see http://www.spaceweather.com/). The corresponding diagram shown in Fig. 2 (left) indicates that in the late nineteenth and early twentieth century similarly long periods of DWNS were recorded. The total solar irradiance level (TSI: i.e. total amount of solar energy measured by Earth-orbiting spacecraft) in 2009 was the lowest since the beginning of space era in the 1950s (http://www.pmodwrc.ch/pmod.php?topic=tsi/composite/SolarC
The solar wind permeating interplanetary space was also affected during the minimum as indicated by the distribution of solar wind velocity in 2009, with a peak at low median value of 340 km/s. In addition, the solar centimetre-wave radio emission at 10.7 cm, which is highly correlated with the total solar X-ray flux (Fröhlich, 2012), was at an extremely low level in 2009, as were sightings of auroras at high latitudes. Therefore, our answer to the question posed is *yes*, at least for the past

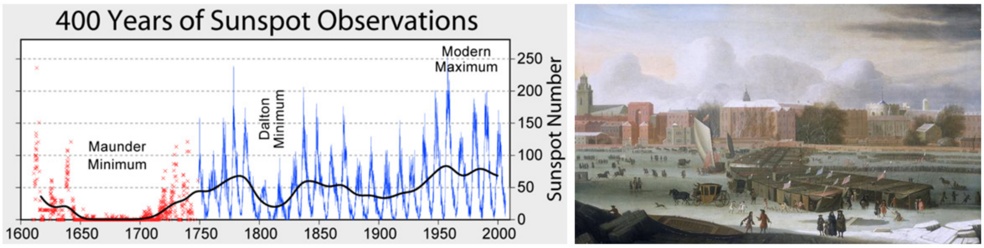


Fig. 2: **Left**: The Maunder minimum in a 400-year history of sunspot numbers (wikipedia) **Right**: A Frost Fair on the River Thames at Temple Stairs, London, January 1684 (Museum of London).

100 years, thus including the last fifty years of the space era. However, solar activity of the new cycle (number 24) eventually resumed, with a slight delay. This was not the case for the solar minimum recorded in the mid-seventeenth century, not long after telescopic recordings of sunspots were first made (see Galileo Project, http://galileo.rice.edu/sci/observations/sunspots.html). A period of virtual absence of sunspot sightings and auroras for tens of years (1645–1715) is now recognized and called after its discoverer the Maunder Minimum – a state of protracted low activity when the conditions in the corona most likely resembled the 2009 minimum. The Maunder Minimum coincided with a "Little Ice Age", during which Europe and North America were subject to bitterly cold winters (Fig. 2 right panel). A definite connection between low sunspot activity and cold winters has not been proved, but some evidence of lower temperatures on Earth occurring at times of low sunspot activity has been claimed.

## 3 SphinX spectrophotometer

SphinX (Gburek et al. (2013), see Fig. 3) was a Polish-built X-ray spectrophotometer on the Russian *CORONAS-Photon* satellite. This instrument was located within the Ultraviolet Telescope TESIS designed at the Lebedev Physical Institute of the Russian Academy of Sciences (Kuzin et al., 2011). *CORONAS-Photon* was launched on 30 January 2009 from the Plesetsk Cosmodrome into a circular ∼550 km altitude, ∼96 minutes, Sun-synchronous orbit with an inclination to the Equator of 82.5°. The spacecraft was pointed at the Sun's disk centre to better than ± three arcminutes. All SphinX raw data are publicly available from http://156.17.94.1/sphinx_catalogue/SphinX_cat_main.html, while the reduced data are given in several pages of the catalogue at http://156.17.94.1/sphinx_l1_catalogue/SphinX_cat_main.html. The SphinX instrument (see Fig. 3) used four silicon PIN detectors (D1, D2, D3, D4 in order of decreasing aperture size), all equipped with thin (12.7 $\mu$m thickness) Be entrance filters blocking solar EUV radiation. The detectors were capable of recording the soft X-ray spectra and photometry. SphinX observed the soft X-ray emission from the entire solar corona in the energy range ∼1 to 15 keV over the period February to November 2009. SphinX was the most sensitive instrument of any taking solar spectra in this soft X-ray range. Its sensitivity exceeded ∼100 times that of the corresponding thresholds of the two XRS detectors (wavelength ranges 1-8 Å and 0.5-4 Å) on the *GOES* X-ray monitoring satellites administered by the US National Oceanic and Atmospheric Administration (NOAA) (see http://www.ngdc.noaa.gov/stp/satellite/goes/doc/GOES_XRS

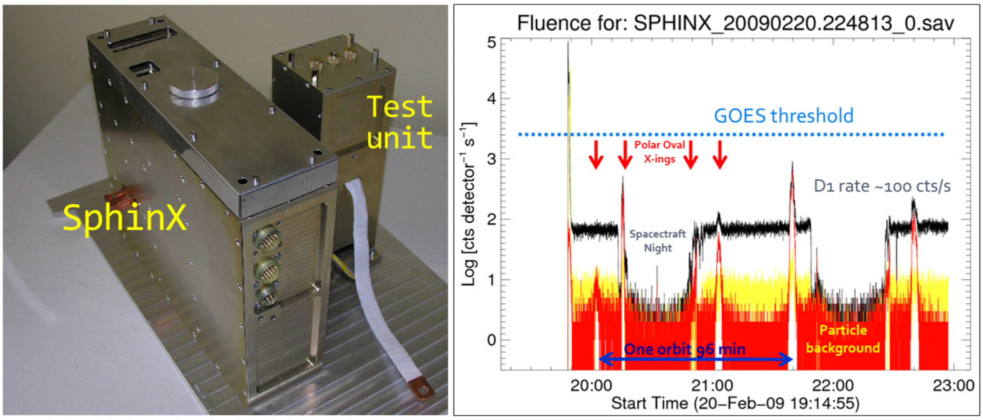


Fig. 3: **Left**: Photograph of SphinX (payload weight 3.5 kg) with its test unit used during instrument calibrations at the BESSY II Berlin synchrotron. **Right**: First recordings of solar soft X-ray fluence showing that the instrument's capability of measuring the Sun's total X-ray emission well below the *GOES* threshold. For the first time it was possible to observe the level of non-active solar emission at the time when no active region was present on the disc. Modulation due to spacecraft orbital motion (spacecraft nights, polar oval crossings and South Atlantic Anomaly transits are clearly visible).

_readme.pdf). This high sensitivity was of crucial importance for observing the solar variability during this period of exceptionally low X-ray emission. In Fig. 4, the light curve characterizing solar X-ray flux variability in the 1-8 Å band of SphinX is shown. Overplotted in blue is the *GOES* record in the same wavelength band. A very good correspondence between the two plots is observed for times when the solar flux was above the *GOES* sensitivity threshold. Each peak seen in the light curve corresponds to a solar flare or micro-flare. More than 1000 such events were recorded, most of them related to the occasional active regions that occurred over this time. The presence of an active region resulted in an increase of X-ray emission above the base-line level corresponding to $\sim 4 \times 10^{-9}$ W m$^{-2}$. This base-line level in the 1-8 Å spectral band is ∼20 times below the threshold of *GOES* XRS (blue line). The variations recorded by SphinX were therefore previously unknown, since the solar X-ray emission in the preceding two minima (between cycles 21/22 and 22/23) was above this threshold. New X-ray luminosity classes need to be introduced to characterize the magnitude of events below the *GOES* threshold: we called these new emission categories S (small) and Q (quiet). They are indicated in Fig. 4 (right axis). The measured base-line solar emission level thus corresponds to class Q4.0. The base-line value can be used to redefine the minimum luminosity of the X-ray emission of the Sun (LRASS) in the energy range 0.1-2.4 keV to the level log (LRASS) = 25.2 (LRASS is in erg s$^{-1}$: see Sylwester et al. (2012)). Compared with nearby X-ray-emitting stars, the Sun in 2009 was inside the lower range of 15% emission population of K and M dwarf stars.

## 4 SphinX and the other instruments measuring solar emission

There were at least six other space instruments taking measurements of solar total radiation and taking images over the 2009 minimum. SphinX was the most sensitive of them. Data from the other instruments support SphinX measurements to a large

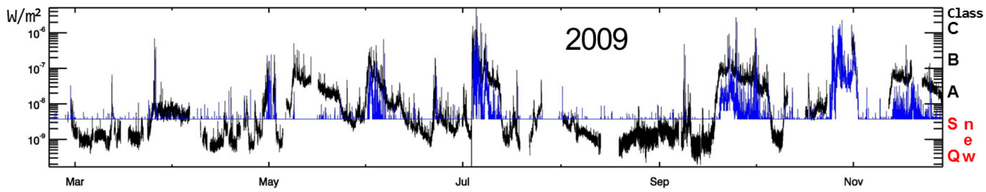


Fig. 4: A full record of SphinX soft X-ray photometry of the Sun in the period February to November 2009. Values of the fluxes were determined in the isothermal approximation from the photon count rates measured in energy bands 1.16-1.5 keV and 1.5-15 keV. The corresponding *GOES* measurements are shown in blue.

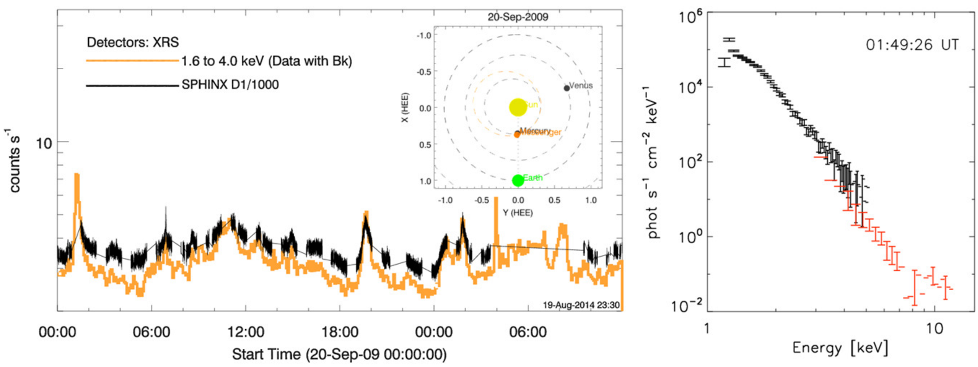


Fig. 5: **Left**: Comparison of soft X-ray light curves recorded by SphinX (black line) and one channel of *MESSENGER* SAX (orange). See the inset for the position of S/C. **Right**: Examples of *RHESSI* and SphinX photon spectra. Black data points with error bars are the SphinX spectrum. *RHESSI* points are shown in red. This comparison was made for the time around the rise phase of a small flare of 18 July 2009 at 01:49:26 UT.

extent by taking measurements not only in different energy (or wavelength) bands, but also from different vantage point. In Fig. 5, we present examples of the light curves observed by SphinX and the SAX X-ray solar monitor aboard *MESSENGER*. SAX (see http://www.nasa.gov/pdf/525164main_MercuryMOI_PK.pdf) is a solar soft X-ray photometer, a part of the SPEX instrument for studies of the surface composition of the planet Mercury. A very good correspondence between SAX and SphinX measurements is evident from Fig. 5. In addition, the *RHESSI* hard X-ray imager (http://hesperia.gsfc.nasa.gov/rhessi2/) spectral ranges slightly overlap with SphinX (see Fig. 5). However, the sensitivity of *RHESSI* is insufficient to measure the Sun's X-ray emission in the absence of active regions. In order to study the spectrum of the coronal emission corresponding to the base-line emission, we accumulated counts for ∼6 hours on 16 September 2009. In Fig. 6 the measured spectrum is shown with that calculated in with an isothermal approximation. Using this isothermal model it is possible adequately to describe the observed spectrum of the non-active-region corona in the range 1.2-3 keV. The derived temperature and emission measure (1.7 MK and $10^{48}$ $cm^{-3}$ respectively) are thus typical average conditions of the solar non-active corona. One may try to look in more details on the distribution of temperatures in the corona. This can most conveniently be done by studying the images of the corona taken in slightly different energy ranges. Routine patrol images taken by the XRT telescope (http://xrt.cfa.harvard.edu/) aboard the *Hinode* solar observatory provide

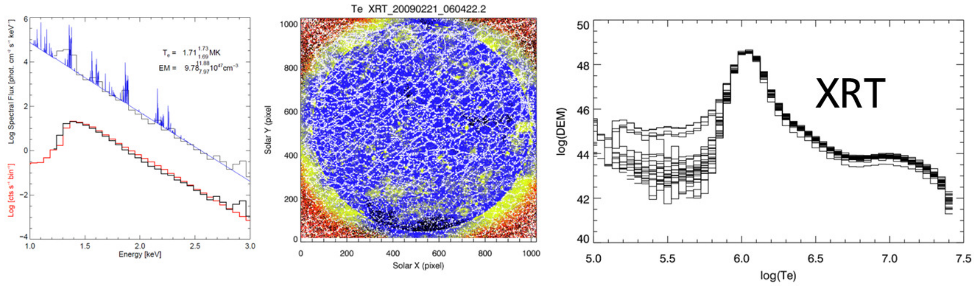


Fig. 6: **Left**: Averaged photon spectrum in the 1-3 keV range (upper histogram) for the time period when the total SphinX D1 count rate was below 110 counts $s^{-1}$. See (Sylwester et al., 2012) for details. **Centre**: An example of temperature map obtained for the base-line level of activity from *Hinode* XRT data on 2009 February 21 06:04 UT. Black, blue, yellow, and red areas correspond to regions with average log(T) = 5.0, > 5.9, > 6.1, >6.4 ranges respectively (T = temperature in Kelvins). The characteristic white network corresponds to contaminated CCD pixels, not used in the analysis. **Right**: So-called quasi-DEM (differential emission measure) distribution as determined for all 27 base-line activity level XRT images observed from February to September 2009.

such opportunity. Ratio of intensity images taken through X-ray filters (known as Thin_poly and Thin_al) can be interpreted in terms of the temperature averaged along the column contributing to the emission in every pixel. The resulting map of temperature distribution is presented in Fig. 6 (center panel). The colours represent plasmas at various temperature ranges. It is seen that the "colder" plasma (in black) fills regions of coronal holes and above, towards the outer corona. Blue regions with T in the range 0.8 - 1.3 MK (i.e. close to an "average" quiet corona temperature) cover most of the disk. The yellow areas corresponding to somewhat hotter emission in the DEM distribution with T in the range 1.3 - 2.5 MK constitute left-overs of the "activated corona", i.e. tiny active regions and bright points. This hotter emission also occupies regions of the inner corona immediately near and above the limb. The red areas represent the hottest emission of the quiet corona where $T > 2.5$ MK. This very hot emission is not evident when projected on the disk, but it overwhelms the outer corona due to line-of-sight integration effects at large distances from the solar surface. This is a new result from a study under preparation at present (Siarkowski et al., 2014). With the aim of better characterizing the overall distribution of plasma in the entire solar corona, the emission measure can be summed in all pixels having the same temperature (to within a given limits). This has been done for the time of the base-line conditions and the result is presented in Fig. 6 (right) where the distribution of such quasi-differential emission measure is presented. From the histogram it is seen that the most of quiet coronal plasma is at a temperature of ~1 MK, but a hot component is definitely present with the temperatures around 10 MK. The presence of this hot component supports a so-called nano-flare coronal heating scenario that has been advanced by some investigators.

## 5 Conclusions

The most recent solar activity minimum of 2008/2009 was unique in the sense of being the longest and deepest in the space era starting in the late 1950s. Levels of X-ray flux during periods when no active regions were visible on the disk were below the sensitivity threshold of all instruments except the Polish SphinX spectrophotometer. SphinX measurements define the lowest X-ray luminosity of the Sun seen as a star, providing the average temperature and emission measure of the minimum-activity corona. However, the XRT soft X-ray images indicate the presence of regions in the corona at temperatures of  10 MK, even during the lowest-activity periods. These results are in direct support of the concept of heating the corona through multiple (millions) of nano-flares releasing small energy parcels through magnetic reconnection higher-up in the corona (100 000 km above the photosphere). There are some indications that the next solar minimum, expected in 2017 or 2018, may have similarly low levels of X-ray emission.

*Acknowledgements.* The success of SphinX Polish spectrophotometer was possible through the grant N N203 381736 of Polish National Science Centre. The present contribution has been set under umbrella of the grant UMO-2011/01/M/ST9/06096 of this Agency.

## References

de Toma, G., *Evolution of Coronal Holes and Implications for High-Speed Solar Wind During the Minimum Between Cycles 23 and 24*, Sol. Phys. **274**, 195 (2011)

Fröhlich, C., *Total Solar Irradiance Observations*, *Surveys in Geophysics* **33**, 453 (2012)

Gburek, S., et al., *SphinX: The Solar Photometer in X-Rays*, Sol. Phys. **283**, 631 (2013)

Habbal, S. R., et al., *Total Solar Eclipse Observations of Hot Prominence Shrouds*, ApJ **719**, 1362 (2010)

Hathaway, D. H., *The Solar Cycle*, *Living Reviews in Solar Physics* **7**, 1 (2010)

Kuzin, S. V., et al., *The TESIS experiment on the CORONAS-PHOTON spacecraft*, *Solar System Research* **45**, 162 (2011)

Siarkowski, M., et al. (2014), in preparation

Sylwester, J., et al., *SphinX Measurements of the 2009 Solar Minimum X-Ray Emission*, ApJ **751**, 111 (2012)